ADVANCED MATERIALS

DOI: 10.1002/adma.200702343

# High Efficiency and Small Roll-Off Electrophosphorescence from a New Iridium Complex with Well-Matched Energy Levels**

By *Zhi Qiang Gao*, *Bao Xiu Mi*,* *Hoi Lam Tam*, *Kok Wai Cheah*, *Chin Hsin Chen*, *Man Shing Wong*, *Shuit Tong Lee*, and *Chun Sing Lee*

It is well-known that, under electrical excitation, singlet and triplet excitons will be formed in organic light-emitting diodes (OLEDs) in the ratio of approximately 1 to 3 in the organic layers, where recombination of opposite charges occurs. The harvesting of triplet excitons for emission (termed as phosphorescence) cannot be obtained in common organic compounds because of the spin-forbidden rule. Thus, metal complexes, possessing the spin-orbit coupling effect caused by the heavy metal, are commonly used as phosphorescent emitters. Hence, intensive efforts have been made towards the development of metal complexes with different colors.[1–8] Phosphorescent OLEDs (PhOLEDs) with peak efficiencies as high as 8.5 % (or 8.5 lm $W^{-1}$) for blue,[2] 19.2 % (or 70 lm $W^{-1}$) for green,[9] and 11 % (or 11.2 lm $W^{-1}$) for red[3] have been reported in the literature. On the other hand, PhOLEDs, in spite of having the ability of harvesting triplet energy that can result in high efficiency, are usually characterized by high roll-off in efficiency with increasing current density.[2,9–11] Typically, the external quantum efficiency (EQE) declines sharply at current densities above 20 mA $cm^{-2}$, which is the practical driving condition for passive-matrix OLEDs (PMOLEDs). Furthermore, high driving voltages are usually observed in these devices, which can result in low power efficiencies.[12,13] As with the issues of generally high roll-off and driving voltage in PhOLEDs, it has been found that the roll-off was attributed to the triplet–triplet (T–T) annihilation[14,15] and/or the field-induced exciton dissociation[16,17] when there was a high density of triplet excitons with long lifetimes. The high driving voltage is supposed to be caused by two factors: one is the deep and strong charge traps caused by the doped iridium complex in the emitting layer;[12,13] the second is related to the highest occupied molecular orbital (HOMO), which transfers holes, and the lowest unoccupied molecular orbital (LUMO), which transfers electrons, of materials used. In PhOLEDs, to match the triplet energy level of the dopant for exothermic energy transfer, high bandgap host materials are usually required. So the difference in HOMO levels and/or LUMO levels between the carrier transporting and the emitting layers is usually large, making charge injection into the emitting layer energetically unfavorable and thus leading to high driving voltage.[18]

To achieve high efficiency PhOLEDs with the characteristics of small roll-off and low driving voltage, it is believed that both high-efficiency phosphorescent materials and the practical construction of devices are needed. Of primary importance in device architectures is that the hole/electron injection barrier from the hole/electron transport layer to the emitting layer should be small, which will favor charge injection and avoid high driving voltage. Secondly, the density of triplet excitons should be low enough for the purpose of minimizing T–T exciton annealing. This criterion can be achieved by evenly distributing excitons in the bulk emission layer rather than having excitons located only at the narrow interface sites. Finally, the confinement of the exciton within the phosphorescent material layer is also important. If the exciton is not produced in and/or drifts out of the phosphorescent emitter layer with bias variation, the resulting singlet emission from other materials would not only definitely lead to impurity of color but also result in further roll-off in efficiency, because singlet excitons only take up 25 % of the total number of excitons formed by electrical excitation.

In this work, we report a new homoleptic cyclometalated iridium triplet green emitter based on a phenylpyridazine ligand. The complex possesses good thermal stability, strong

[*] Dr. B. X. Mi
Institute of Advanced Materials (IAM)
Nanjing University of Posts and Telecommunications
66 Xin Mofan Road, Nanjing (P.R. China)
E-mail: iambxmi@njupt.edu.cn
Dr. Z. Q. Gao, Dr. H. L. Tam, Prof. K. W. Cheah
Centre for Advanced Luminescence Materials
Hong Kong Baptist University
Waterloo Road, Kowloon Tong, Hong Kong (P.R. China)
Prof. C. H. Chen
Display Institute, Microelectronics and Information Systems Research Center
National Chiao Tung University
Hsinchu, Taiwan 300 (Taiwan)
Prof. M. S. Wong
Department of Chemistry
Hong Kong Baptist University
Waterloo Road, Kowloon Tong, Hong Kong (P.R. China)
Prof. S. T. Lee, C. S. Lee
Center of Super-Diamond and Advanced Films (COSDAF) and Department of Physics and Materials Science
City University of Hong Kong
Tat Chee Avenue, Kowloon, Hong Kong (P.R. China)

[**] This work was supported by a Hong Kong Baptist University Faculty research grant (FRG/05-06/I-48), a Hong Kong Innovation and Technology Commission Guangzhou-Hong Kong Industrial Support Grant (ITC/05-06/02), and financial support from Nanjing University of Posts and Telecommunications (NY207013).

green phosphorescence, and well-matched energy levels with the commonly used host, 4,4′-*N*,*N*′-dicarbazole-biphenyl (CBP), in PhOLEDs. The complex has been fully characterized and the device physics have been investigated. The blue emission from our first-attempt PhOLED device is interpreted with the assistance of an energy-level diagram. And with an improved device configuration, this blue emission is totally eliminated. We found that, in addition to the strong phosphorescent feature of the new material, the well-matched energy levels of the new phosphorescent material with the host (CBP) and the insertion of the energy level buffer layer were crucial for obtaining the high EQE and power efficiency, and the small roll-off in efficiency in our device.

The green-light-emitting $Ir^{III}$ complex, tris[3,6-bis(phenyl)-pyridazinato-$N^1$,$C^{2'}$]iridium $(IrBPPya)_3$, can be synthesized in moderate yield (58 %) by a two-step reaction, as shown in Scheme 1. In the first step, *trans*-1,2-dibenzoylethylene transformed thermally into its cis intermediate isomer,[19] which further reacted with hydrazine to yield 3,6-bis(phenyl)pyridazine (BPPya) through an intramolecular ring-closure reaction. $Ir(BPPya)_3$ was obtained by refluxing the above ligand and tris(acetylacetonato)-iridium(III) in degassed glycerol.[20] Purification of the precipitate by flash-chromatography yielded the homoleptic cyclometalated iridium complex as an air-stable orange powder in high purity. $^1$H NMR spectroscopy, elemental analyses, and mass spectrometry (MS) results are consistent with the proposed structure. $Ir(BPPya)_3$ shows excellent thermal behavior, with a melting point of 438.1 °C, as determined by differential scanning calorimetry (DSC), and a 5 %-weight-loss temperature of 439 °C, as revealed by thermogravimetric analysis (TGA). It is strongly believed that the nature of the 5 % weight loss is due to sublimation.[21] Furthermore, it can be thermally evaporated under vacuum with a very stable deposition rate.

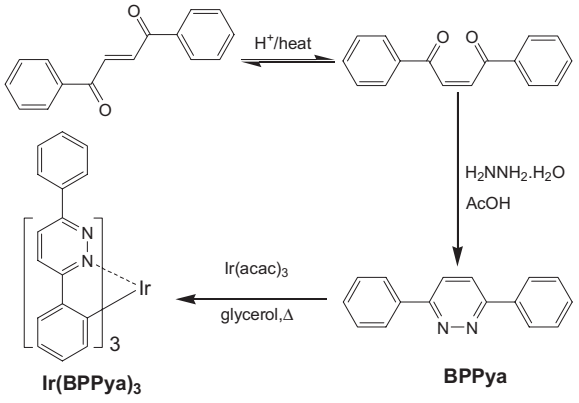


**Scheme 1.** Synthesis of $Ir(BPPya)_3$.

By focusing on the chelated N atom in the ligand, it can be seen that the steric hindrance originating from the adjacent N atom is small because this adjacent N is bonded in the rigid six-member ring and has no other atom attached to it. So the metal–ligand bonding between the chelated N atom and the metal is strong, resulting in a large first-order spin-orbit coupling term in the $T_1 \rightarrow S_0$ transition by the direct involvement of the metal $d_\pi$ orbital. This leads to efficient mixing of the singlet and triplet excited states, which would result in a drastic decrease in the radiative lifetime and, hence, the possibility of increasing the quantum yield.[2] Consistent with the above prediction, $Ir(BPPya)_3$ has an observed radiative lifetime of 1.69 μs and a phosphorescent quantum yield ($\Phi_p$) of 0.8 relative to $Ir(ppy)_3$ ($\Phi_p$ = 0.40),[22] which is estimated from a 7 % $Ir(BPPya)_3$-doped CBP film and an ambient toluene solution ($1\times10^{-5}$ M), respectively.

Figure 1 shows both absorption and photoluminescence (PL) spectra in an ambient toluene solution ($1\times10^{-5}$ M). By comparison to the absorption of the free ligand, the absorption band located at 284 nm can be assigned to spin-allowed

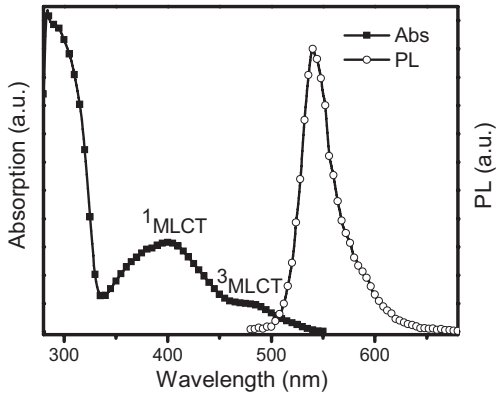


**Figure 1.** UV-vis absorption and photoluminescence spectra of $Ir(BPPya)_3$ in toluene ($10^{-5}$ M) (excitation @ 440 nm; MLCT: metal–ligand charge transfer).

$^1(\pi-\pi^*)$ transitions on the cyclometalating ligand, which has the highest absorption ability (molar absorption coefficient, $\varepsilon$ = 50 000 $M^{-1}$ $cm^{-1}$). The bands at 400 nm ($\varepsilon$ = 14 000 $M^{-1}$ $cm^{-1}$) and ~471–475 nm ($\varepsilon$ = 4500 $M^{-1}$ $cm^{-1}$) can be assigned to the metal–ligand charge transfer (MLCT) of the spin-allowed transition ($^1$MLCT) and a mixture of spin-forbidden bands of $^3$MLCT with ligand-centered $^3(\pi-\pi^*)$ transitions, respectively. The relatively high extinction coefficient of these triplet bands indicates the efficient spin-orbital coupling that can result in highly efficient phosphorescent emission.[6] $Ir(BPPya)_3$ emits intensively with green phosphorescence peaked at 541 nm, which can be assigned to a predominantly $^3$MLCT state radiative transition.[23,24]

To gain guidance for device construction, the energy levels of $Ir(BPPya)_3$ were analysed by cyclic voltammetry (CV) in a dimethylformamide (DMF) solution, using Ag/AgCl as reference electrode. Reversible oxidation at 1.03 V and quasireversible reduction at –1.88 V were revealed. The HOMO and LUMO levels, deduced from these data by a previously described method,[25] are 5.75 and 2.84 eV relative to vacuum

  

ADVANCED MATERIALS

level, respectively. It can be predicted that by using CBP as host (HOMO: 6.0 eV, LUMO: 2.9 eV[26]), hole transfer from CBP to $Ir(BPPya)_3$ is energetically favorable and $Ir(BPPya)_3$ will form shallow positive charge traps in the CBP host because there exists a potential of 0.25 eV (6.0 minus 5.75 eV) for hole transfer from CBP to $Ir(BPPya)_3$. Furthermore, the barrier for electron transfer in this direction is also very small (only 0.06 eV = 2.9–2.84). Obviously, CBP is a good host for $Ir(BPPya)_3$.

Devices were fabricated with the structure of ITO/NPB (60 nm)/$Ir(BPPya)_3$-doped CBP (40 nm)/BPhen (20 nm)/LiF (1 nm)/Al (100 nm), in which $Ir(BPPya)_3$ worked as the phosphorescent dopant emitter, CBP as the host material, and BPhen was used to serve as the electron-transporting layer.[27] Here, ITO is indium tin oxide, NPB is *N*,*N*′-bis-(1-naphthyl)-*N*,*N*′-diphenyl,1,1′-biphenyl-4,4′-diamine, and BPhen is 4,7-diphenyl-1,10-phenanthroline. It was found that the best performance was achieved by the device with an $Ir(BPPya)_3$ doping concentration of 7 % (D1). However, even at high doping concentration, such as 7 % in D1, blue-light emission, which supposedly originates from NPB by the carrier/exciton drifting mechanism,[28] existed (see Fig. 3a, below). By examining the energy levels layer by layer (as shown in Fig. 2), it can be seen that the barrier for electron injection into CBP is 0.1 eV,

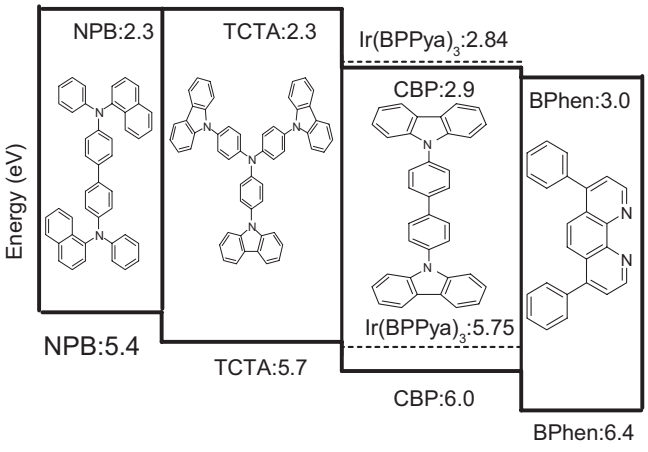


**Figure 2.** HOMO (lower values) and LUMO (upper values) energy levels [eV] of $Ir(BPPya)_3$ superimposed onto the energy diagram of the OLED device D2 (TCTA: 4,4′,4″-tri(*N*-carbazolyl)triphenylamine).

and that for further moving to the NPB layer is 0.6 eV; meanwhile, the hole-injection barrier from NPB into CBP is as large as 0.6 eV. This means that at the NPB/CBP interface, the energy barrier for electron to NPB and that for hole to CBP are equal. Thus, recombination will mainly occur at the NPB/CBP interface, either on NPB or CBP. As a result, in addition to $Ir(BPPya)_3$ emission by direct charge trapping on $Ir(BPPya)_3$ and/or energy transfer from CBP at the NPB/CBP interface, NPB excitons at the NPB/CBP interface will give NPB emission. Having the emission contribution from fluorescence of NPB means sacrificing the triplet excitons, so the maximum efficiency of D1 is not high (about 20 cd $A^{-1}$). Furthermore, the large barrier (0.6 eV) for hole injection into CBP results in a high driving voltage, as presented in the device D1 (see Table 1).

**Table 1.** Performance data of devices D1 and D2.

| No. [a] | Voltage [V] | | | Current efficiency [cd $A^{-1}$] | | |
|---|---|---|---|---|---|---|
| | 1 mA $cm^{-2}$ | 10 mA $cm^{-2}$ | 70 mA $cm^{-2}$ | 1 mA $cm^{-2}$ | 10 mA $cm^{-2}$ | 70 mA $cm^{-2}$ |
| D1 | 5.5 | 7.9 | 10.5 | 16.1 | 13.9 | 12.0 |
| D2 | 4.9 | 6.3 | 8.7 | 52.2 | 48.7 | 40.4 |

[a] D1: ITO/NPB (60 nm)/CBP:7 % $Ir(BPPya)_3$ (40 nm)/Bphen (20 nm)/LiF/Al; D2: ITO/NPB (52 nm)/TCTA (8 nm)/CBP:7 % $Ir(BPPya)_3$ (40 nm)/Bphen (20 nm)/LiF/Al.

These problems are supposed to be solved by insertion of a hole-transporting material with the required energy levels between NPB and CBP, which can reduce the hole-injection barrier to CBP. Hence, TCTA,[29] 4,4′,4″-tri(N-carbazolyl)triphenylamine, was chosen, acting as a carrier/exciton confinement component. Figure 2 shows the energy diagram of the device D2 with the structure of ITO/NPB (52 nm)/TCTA (8 nm)/7 % $Ir(BPPya)_3$ in CBP (40 nm)/BPhen (20 nm)/LiF (1 nm)/Al (100 nm). With TCTA, the recombination zone will be located at the CBP layer adjacent to the interface of TCTA/CBP because there is only a 0.3 eV barrier for hole injection from TCTA to CBP, smaller than the electron-injection barrier of 0.6 eV from CBP to TCTA. Such a device energy structure will significantly reduce the exciton leakage into NPB. Meanwhile, because $Ir(BPPya)_3$ forms a shallow trap in the CBP host, the positive charges, which can eventually convert to excitons by recombination, will not only reside on the guest emitter at the interface but also on the host. Thus, in addition to direct carrier recombination on the guest, which is the dominant mechanism in most iridium-complex-doped CBP PhOLEDs,[30,31] there exists energy transfer from host to guest. The excitons, formed on the host CBP molecules at the recombination zone, can be transferred to the guest $Ir(BPPya)_3$ molecules located far away from the TCTA/CBP interface via long-range energy transfer. This will result in low exciton density and uniform distribution of excitons in the whole emitting layer, significantly reducing T–T annihilation. Thus, small roll-off in EQE at high current density is achieved.

Figure 3 shows the device performances of D1 and D2. Unlike D1, when a TCTA layer was inserted, the electroluminescence (EL) spectra (Fig. 3a) beared close resemblance to the solution PL of $Ir(BPPya)_3$, and only green phosphor emission was observed. Moreover, the EL spectra did not consist of any other residual emission from the host and/or adjacent layers even at high current density, indicating complete energy and/or charge transfer from the host exciton to the triplet dopant emitter upon electrical excitation. Meanwhile, it can be seen from Figure 3b and Table 1 that, with the TCTA layer, the driving voltage of D2 was significantly reduced.

  

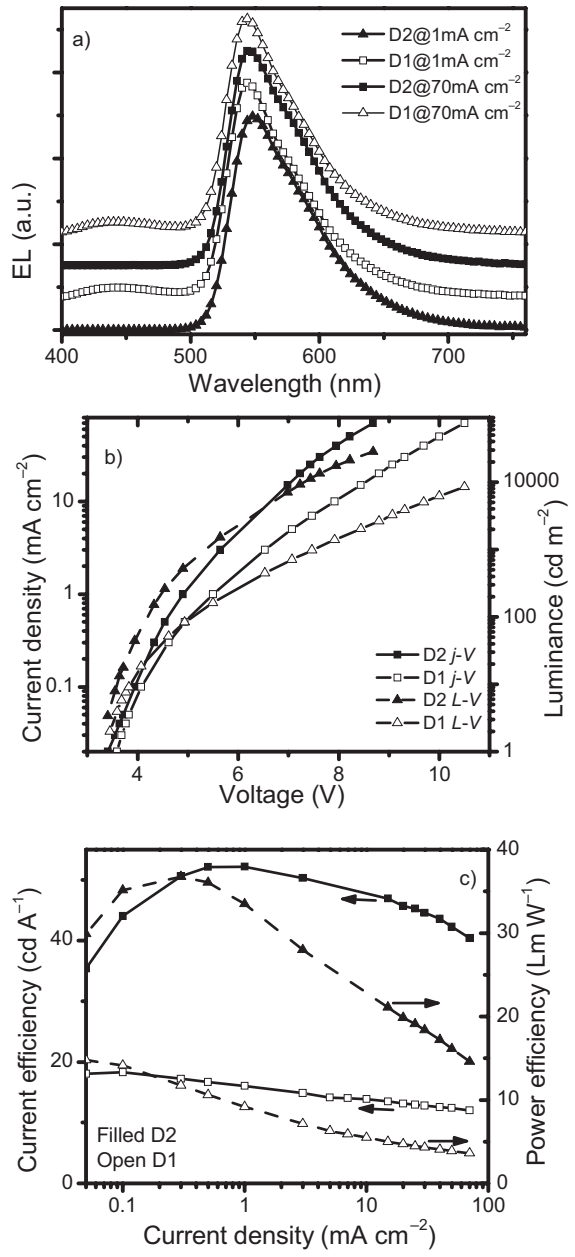


**Figure 3.** Device performances of D1 and D2: a) electroluminescence (EL); b) current density–voltage–luminance (*j–V–L*); c) current efficiency and power efficiency versus current density.

The turn-on voltage (defined as the bias at a brightness of 1 cd m$^{-2}$) was 3.3 V for D2 and 3.5 V for D1. The driving voltage of D2 was 6.3 V for a current density of 10 mA cm$^{-2}$ and 8.7 V for a current density of 70 mA cm$^{-2}$, while the counterparts for D1 were 7.9 V and 10.5 V, respectively. Figure 3c shows the current efficiency and power efficiency versus current density for D1 and D2. Compared to D1 where the TCTA layer was absent, the efficiencies are dramatically increased. D2 has a maximum EQE of 14.6 % at about 1 mA cm$^{-2}$, corresponding to a current efficiency of 52 cd A$^{-1}$ and a power efficiency of 33.5 lm W$^{-1}$. A measure of the roll-off can be defined as the percentage drop in $\eta_{EL}$ at a given field ($F$) or current density ($j$) with a reference to its maximum value $\eta_{EL}$(max), that is, roll-off = $\{[\eta_{EL}(\max) - \eta_{EL}(F,j)]/\eta_{EL}(\max)\}$, where $\eta_{EL}$ represents current efficiency or EQE.[16] The roll-off for D2 was 13 % at 20 mA cm$^{-2}$ and 23 % at 70 mA cm$^{-2}$. These values are significantly lower compared to other triplet devices,[2,9–11] suggesting that the T–T annihilation may not be a critical quenching mechanism in our Ir(BPPya)$_3$/CBP device configuration.

In summary, we have reported the synthesis, characterization, and device performance investigation of a new phosphorescent material, Ir(BPPya)$_3$. Through the study of the device physics with Ir(BPPya)$_3$, we demonstrate that T–T annealing in PhOLED can be avoided if the energy levels of the host and the phosphorescent dopant are closely matched. And the emission from other materials at the interface can also be confined via the energy-level buffer layer. These insights are helpful to produce a practical design scheme for both new PhOLED materials and new device structures. The present results show that Ir(BPPya)$_3$ is a promising material in terms of both efficiency and thermal stability. Based on Ir(BPPya)$_3$, a device with a maximum external quantum efficiency of 14.6 %, corresponding to a current efficiency of 52 cd A$^{-1}$ and a power efficiency of 33.5 lm W$^{-1}$, has been obtained. Remarkably, besides the high efficiency, the present device has a strikingly small roll-off in EQE with increasing current compared to other PhOLEDs.

## *Experimental*

*Synthesis of 3,6-Bis(phenyl)pyridazine (BPPya)*: *trans*-1,2-Dibenzoylethylene (formula weight, FW = 236.27; 1.5 g, 6.35 mmol) was dissolved in acetic acid (40 mL) by heating. After cooled down to room temperature, an excess amount of hydrazine monohydrate (25 mL) was added dropwise. The reaction mixture was kept stirred at room temperature for another hour, and then refluxed overnight. After cooling down, the solution was poured into ice to obtain a white precipitate. Subsequent recrystallization from chloroform yielded the product (0.57 g, 38 %) [32]. m.p. 222 °C. MS: *m/z* 233.0 (M+1).

*Synthesis of Ir(BPPya)$_3$*: The starting material BPPya (FW = 232.28; 546.6 mg, 2.35 mmol) and Ir(acac)$_3$ (FW = 489.54, Hacac: acetylacetone; 289.8 mg, 0.592 mmol) were dissolved in degassed glycerol (10 mL). Dark-orange colored products precipitated out gradually upon reflux at 220 °C in a nitrogen environment for 10 h. The precipitate was collected by filtration, washed with hexane and ether, and finally dried in vacuum. It was then purified by flash-chromatography with a silica gel column using dichloromethane as an eluent. Addition of methanol into the solution followed by heating to boil to evaporate the dichloromethane resulted in precipitation of the product as an orange-colored solid (1.2 g, 58 %). m.p. 438.1 °C; $^1$H NMR (300 MHz, DMSO-d$_6$, d): 8.44 (d, $J$ = 9.1 Hz, 3H), 8.27 (d, $J$ = 9.1 Hz, 3H), 7.81–7.84 (m, 3H), 7.62–7.65 (m, 6H), 7.24 (t, $J$ = 7.3 Hz, 3H), 7.12–7.15 (m, 3H), 7.03 (t, $J$ = 7.8 Hz, 6H), 6.87–6.93 (m, 6H); MS: *m/z* 887.0 (M+1); Anal. Calcd. for $C_{48}H_{33}N_6Ir$: C, 65.06; H, 3.72; N, 9.48. Found: C, 65.03; H, 3.67; N, 9.70.

*OLED Fabrication and Measurements*: OLEDs were fabricated using a vacuum thermal evaporation chamber with a base pressure of $1\times10^{-6}$ torr (1 torr = 133.3 Pa). All the materials were deposited in one pump-down. Two shadow masks were used to define the deposition areas for the organic and metal cathode. *j–V–L* characteristics and EL spectra of the device were measured with a computer-con-

  

ADVANCED MATERIALS

trolled DC power supply and a Spectrascan PR650 photometer at room temperature. The emission area of the devices was 0.1 $cm^2$, as defined by the overlapping area of the anode and the cathode.

Received: September 15, 2007
Revised: October 24, 2007
Published online: January 29, 2008

[1] W. Y. Wong, C. L. Ho, Z. Q. Gao, B. X. Mi, C. H. Chen, K. W. Cheah, Z. Y. Lin, *Angew. Chem. Int. Ed.* **2006**, *45*, 7800.
[2] C.-H. Yang, Y.-M. Cheng, Y. Chi, C.-J. Hsu, F.-C. Fang, K.-T. Wong, P.-T. Chou, C.-H. Chang, M.-H. Tsai, C.-C. Wu, *Angew. Chem. Int. Ed.* **2007**, *46*, 2418.
[3] J. Huang, T. Watanake, K. Ueno, Y. Yang, *Adv. Mater.* **2007**, *19*, 739.
[4] C. S. K. Mak, A. Hayer, S. I. Pascu, S. E. Watkings, A. B. Holmes, A. Koehler, R. H. Friend, *Chem. Commun.* **2005**, 4708.
[5] S.-C. Lo, N. A. H. Male, J. P. J. Markham, S. W. Magennis, P. L. Burn, O. V. Salata, I. D. W. Samuel, *Adv. Mater.* **2002**, *14*, 975.
[6] S. Lamansky, P. Djurovich, D. Murphy, F. Abdel-Razzaq, H.-E. Lee, C. Adachi, P. E. Burrows, S. R. Forrest, M. E. Thompson, *J. Am. Chem. Soc.* **2001**, *123*, 4304.
[7] M. A. Baldo, D. F. O'Brien, Y. You, A. Shoustikov, S. Sibley, M. E. Thompson, S. R. Forrest, *Nature* **1998**, *395*, 151.
[8] P.-T. Chou, Y. Chi, *Chem. Eur. J.* **2007**, *13*, 380.
[9] M. Ilkai, S. Tokito, Y. Sakamoto, T. Suzuki, Y. Taga, *Appl. Phys. Lett.* **2001**, *79*, 156.
[10] S.-J. Yeh, M.-F. Wu, C.-T. Chen, Y.-H. Song, Y. Chi, M.-H. Ho, S.-F. Hsu, C. H. Chen, *Adv. Mater.* **2005**, *17*, 285.
[11] S. Tokito, T. Iijima, Y. Suzuri, H. Kita, T. Tsuzuki, F. Sato, *Appl. Phys. Lett.* **2003**, *83*, 569.
[12] M. H. Lu, M. S. Weaver, T. X. Zhou, M. Rothman, R. C. Kwong, M. Hack, J. J. Brown, *Appl. Phys. Lett.* **2002**, *81*, 3921.
[13] M. A. Baldo, S. Lamansky, P. E. Burrows, M. E. Thompson, S. R. Forrest, *Appl. Phys. Lett.* **1999**, *75*, 4.
[14] C. Adachi, M. A. Baldo, S. R. Forrest, *J. Appl. Phys.* **2000**, *87*, 8049.
[15] M. A. Baldo, C. Adachi, S. R. Forrest, *Phys. Rev. B* **2000**, *62*, 10 967.
[16] M. Cocchi, V. Fattori, D. Virgili, C. Sabatini, P. D. Marco, M. Maestri, J. Kalinowski, *Appl. Phys. Lett.* **2004**, *84*, 1052.
[17] J. Kalinowski, M. Cocchi, P. D. Marco, W. Stampor, G. Giro, V. Fattori, *J. Phys. D: Appl. Phys.* **2000**, *33*, 2379.
[18] T. Tsuzuki, S. Tokito, *Adv. Mater.* **2007**, *19*, 276.
[19] R. Singh, A. S. Hay, *Macromolecules* **1992**, *25*, 1025.
[20] K. Dedeian, P. I. Djurovich, F. O. Garces, G. Carlson, R. J. Watts, *Inorg. Chem.* **1991**, *30,* 1685.
[21] L. S. Sapochak, A. Padmaperuma, N. Washton, F. Endrino, G. T. Schmett, J. Marshall, D. Fogarty, P. E. Burrows, S. R. Forrest, *J. Am. Chem. Soc.* **2001**, *123*, 6300.
[22] K. A. King, P. J. Spellane, R. J. Watts, *J. Am. Chem. Soc.* **1985**, *107*, 1431.
[23] M. G. Colombo, T. C. Brunold, T. Riedener, H. U. Gudel, M. Fortsch, H. B. Burgi, *Inorg. Chem.* **1994**, *33*, 545.
[24] M. G. Colombo, A. Hauser, H. U. Gudel, *Inorg. Chem.* **1993**, *32*, 3088.
[25] M. R. Andersson, M. Berggren, O. Inganäs, G. Gustafsson, J. C. Gustafsson-Carlberg, D. Selse, T. Hjertberg, O. Wennerström, *Macromolecules* **1995**, *28*, 7525.
[26] I. G. Hill, A. Kahn, *J. Appl. Phys.* **1999**, *86*, 4515.
[27] S. Okada, K. Okinaka, H. Iwawaki, M. Furugori, M. Hashimoto, T. Mukaide, J. Kamatani, S. Igawa, A. Tsuboyama, T. Takiguchi, K. Ueno, *Dalton Trans.* **2005**, 1583.
[28] V. Adamovich, J. Brooks, A. Tamayo, A. M. Alexander, P. I. Djurovich, B. W. D'Andrade, C. Adachi, S. R. Forrest, M. E. Thompson, *New J. Chem.* **2002**, *26*, 1171.
[29] Y. J. Xia, J. Lin, C. Tang, K. Yin, G. Y. Zhong, G. Ni, B. Peng, F. X. Gan, W. Huang, *J. Phys. D: Appl. Phys.* **2006**, *39*, 4987.
[30] A. J. Makinen, I. G. Hill, Z. H. Kafafi, *J. Appl. Phys.* **2002**, *92*, 1598.
[31] M. A. Baldo, S. R. Forrest, *Phys. Rev. B* **2000**, *62*, 10 958.
[32] M. Gnanadeepam, S. Selvaraj, S. Perumal, S. Renuga, *Tetrahedron* **2002**, *58*, 2227.

  